IEEE Access
Multidisciplinary | Rapid Review | Open Access Journal

Received October 28, 2021, accepted November 20, 2021, date of publication November 23, 2021,
date of current version December 2, 2021.

*Digital Object Identifier 10.1109/ACCESS.2021.3130319*

# An Ultralight High-Directivity Ceramic Composite Lens Antenna for 220–330 GHz

**MIKKO KOKKONEN[1], ALI GHAVIDEL[1], NUUTTI TERVO[2], (Member, IEEE), MIKKO NELO[1], SAMI MYLLYMÄKI[1], AND HELI JANTUNEN[1]**

[1]Microelectronics Research Unit, University of Oulu, 90014 Oulu, Finland
[2]Centre for Wireless Communications, University of Oulu, 90014 Oulu, Finland

Corresponding author: Mikko Kokkonen (mikko.kokkonen@oulu.fi)

This work was supported by the Academy of Finland 6Genesis Flagship under Grant 318927.

**ABSTRACT** This work presents the characterization of Lithium molybdenum oxide ($Li_2MoO_4$, LMO) hollow glass microspheres (HGMS) ceramic composite from 0.1 to 1 THz and an associated bullet shaped lens used with WR3.4 for 220-330 GHz band. LMO-HGMS had permittivity of 1.18 and loss tangent of 0.003 at 300 GHz. The calculated reflectivity for the LMO-HGMS-air interface was 0.2 %. The fabricated bullet lens weighed 5 grams and was characterized using an experimental measurement system. The lens was measured to have a focus spot of diameter 1.5 mm. Simulated results showed the lens to operate with a WR3.4 waveguide having a gain of 27.5 dBi with a narrow beam width of 1-degree, 18 dB sidelobe level (SLL), 40% Fractional Beam Width (FBW), and −13 dB $S_{11}$ over the broadband 220-330 GHz.

**INDEX TERMS** 6G, composite materials, dielectrics, lens measurement, low permittivity materials, terahertz materials.

## I. INTRODUCTION

The sub-terahertz (sub-THz) frequency band receives considerable attention in terms of broadband availability in a number of applications such as telecommunication, imaging, joint communication-sensing, and security [1]–[8]. In the past, sub-THz frequencies have been used in short range imaging systems including automotive and aerospace radars [9], [10].

Future sixth generation (6G) telecommunication networks are required to enable Tbps peak data-rates and 0.1 ms latency by using very wide bandwidths (>10 GHz) [11], [12]. However, the current transceiver technologies are not able to fully comply with 6G network requirements due to their limited transition frequency ($f_T$) [13].

Extensive technology development is required to meet the technical requirements of 6G technology and the development can be categorized into software and hardware levels. At the hardware level, the antenna is one of the key components in any transceiver to enable transmission and reception of sub-THz signals with acceptable radiation efficiency, high gain and spatial filtering properties. Even in short range communications operating at frequencies above 200 GHz, the antenna should offer very high gain to compensate for the high path loss and increased noise level caused by the antenna directivity. It has been estimated that a 350 GHz link would require at least 27 dBi gain for transmitting a signal over three meters to allow for 10 % bandwidth [14].

In the past few years, extensive of research has been performed to develop THz antennas [15]–[18]. Especially in high frequency applications, antenna gain, bandwidth, and efficiency are often the key parameters that need to be improved. However, for commercial systems, low cost, light weight, and small size are often equally important properties to enable the widespread usage of the THz frequencies for various applications in communications, imaging, sensing, and joint-communication sensing [19]–[22].

In antenna technology development there is a typical trade-off between gain and bandwidth. In addition to the circuit technology, material properties such as dielectric permittivity and loss value have a clear impact on the antenna performance, which can determine the antenna loss and, consequently, total propagation efficiency.

Typical used dielectric materials are organic, e.g. Teflon, and inorganic, e.g. silicon [23]. All-Ceramic composites, on the other hand, are useful in electronics as they withstand the high operation temperatures required for the electronics packages, and their dielectric permittivity and loss tangent can also be adjusted by mixing them with other materials [24]–[26].

The associate editor coordinating the review of this manuscript and approving it for publication was Chinmoy Saha.

One of the downsides of manufacturing ceramics has been the requirement for a high sintering temperature, which consumes a lot of energy and therefore raises the manufacturing cost. The invention of the Room Temperature Fabrication (RTF) process enabled ceramic fabrication at room temperature instead of above 400°C. One of such RTF ceramics is lithium molybdenum oxide [27], [28].

In this paper, we present an implementation of a bullet-shaped lens fabricated from LMO-HGMS composite for the frequency range 220-330 GHz. The purpose of using HGMS in the composite is to decrease the dielectric permittivity, thus, advancing the performance of the antenna. In Section II dielectric measurement and lens fabrication of the composite for 220-330 GHz are discussed. Section III presents the lens antenna simulations and its characterization using an experimental measurement setup at 220-330 GHz, especially for 300 GHz. Section IV presents a comparison study and in Section V conclusion are discussed.

## II. FABRICATION AND CHARACTERIZATION OF LMO-HGMS CERAMIC COMPOSITE

The lens material used in this study was ceramic composite, more precisely a mixture of lithium molybdenum oxide ($Li_2MoO_4$, LMO) and hollow glass microspheres (HGMS). Material fabrication was performed using a simple room temperature fabrication method (RTF) which required only mixing the LMO and HGMS materials together, casting them to the mold and waiting for the composite to dry. Materials and methods to fabricate LMO-HGMS composite are explained in detail in the previous article [29].

Dielectric parameters of the composite for 0.1 – 1 THz were measured using a time-domain spectroscopy (Terapulse 4000 by Teraview) method [30]. The measurement results are shown in Fig. 1.

At 300 GHz the real part of the permittivity was 1.18, the imaginary part 0.004 and the loss tangent ($\tan\delta$) 0.003. For the 220-330 GHz broadband, the permittivity and loss tangent were constant and for the full frequency range from 0.1 THz to 1 THz the real part was fairly constant, but the imaginary part started to increase above 500 GHz, indicating higher losses from 500 GHz upwards. The measured values are sufficient for low permittivity and low loss lenses for applications operating in the sub-THz band.

To determine the optimum shape for the lens to be fed with a WR 3.4 waveguide and achieve as high a gain at possible, simulation (CST microwave studio [31]) studies were conducted. First the lens was shaped as a half sphere having a diameter of 30 mm which was located at the end of the WR3.4, and then it was stretched until the gain did not increase any further. The resulting lens was a semi-ellipsoid with a radius of 49.5 mm and having a gain value of 17.5 dBi. The lens was fabricated from the LMO-HGMS using a plastic mold to obtain the required shape. The fabricated and simulated lens are shown in Fig. 2.

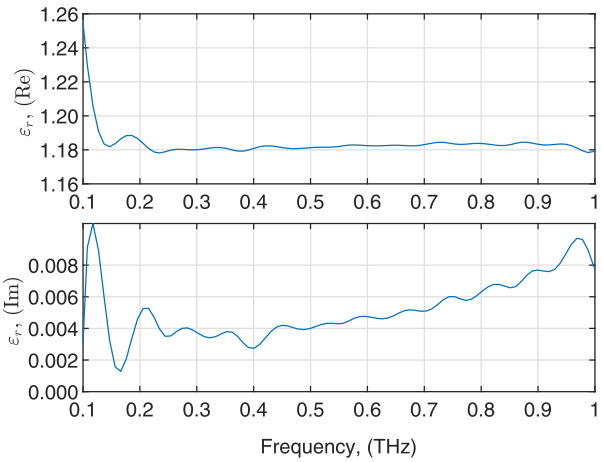


**FIGURE 1.** Measured LMO-HGMS composite dielectric real (Re) and imaginary (Im) parts.

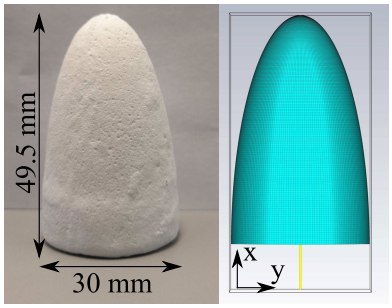


**FIGURE 2.** (At left) picture of the fabricated bullet-shaped LMO-HGMS composite lens weighing 5 grams. The lightness of the composite enables the reduction of the total weight of the transceiver that is useful for many communications and sensing applications. (At right) the simulation model which includes the WR3.4 waveguide model and lens and indicates the direction of the coordinate axes.

## III. LENS ANTENNA SIMULATIONS AND EXPERIMENTAL LENS MEASUREMENT SYSTEM

### A. SIMULATED LENS FOCAL POINT AND RADATION PATTERN

The front focal length (FFL) of the lens at 300 GHz was determined by plane wave simulation (electric field strength, E = 1 V/m). The wave was propagated through the lens entering from the flat side, Fig. 3, and it focused the wave at 21 mm distance from its curved surface.

Because the plane wave simulation indicated that the lens had FFL of 21 mm, positioning the lens directly at the end of the waveguide was not considered the most optimal position. Thus, the second simulation was conducted and the lens was moved from 0 to 25 mm by 1 mm steps from the waveguide to find its optimum location.

The simulated gain at 300 GHz increased from 17.5 dBi to its maximum of 27.5 dBi at 21 mm distance and the radiation pattern of the bullet lens antenna is shown in Fig. 4. The proposed lens waveguide combination had a gain of 27.5 dBi

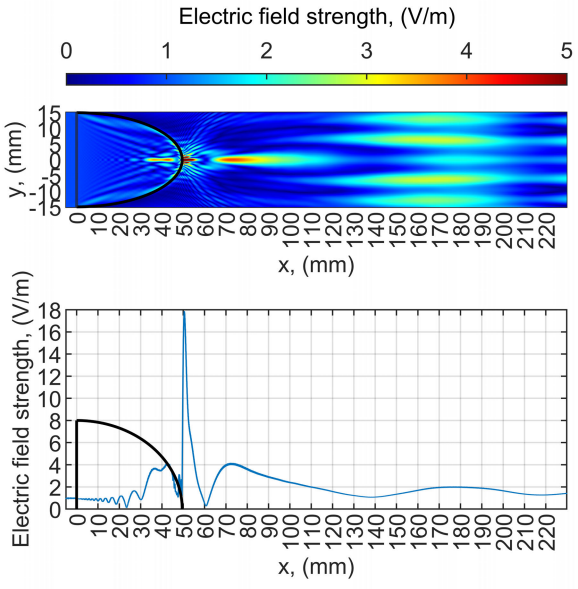


**FIGURE 3.** Simulated E-field of bullet lens at xy-plane and E-field strength along the x-axis. The wave propagates from left to right and focuses at front of the lens, 21 mm from the lens curved surface.

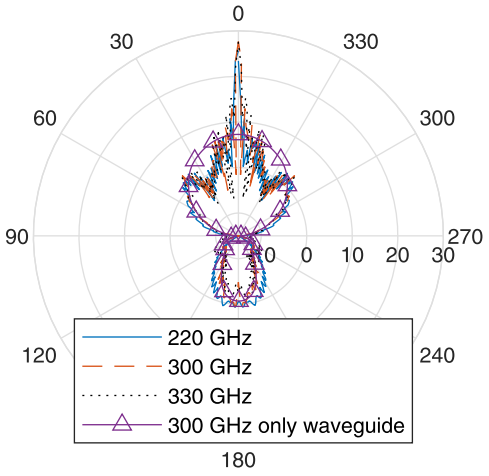


**FIGURE 4.** Simulated radiation pattern of the bullet lens when the lens was at 21 mm distance from the antenna. Scale is in dBi.

with a very narrow main lobe (1°) and 18.8 dB SLL at 300 GHz. For the 220 and 330 GHz: main lobe was 2.1 and 0.7 degrees, SLL was 14.0 dB and 16.0 dB and gain 26.6 dBi and 27.5 dBi, respectively.

Simulated near field and phase are presented for two main scenarios (Fig. 5). When the lens was directly attached to the antenna (Fig. 5(a)), most of the radiation went through the lens sides leading to reduced field strength. However, when the lens was moved to the 21 mm distance from the waveguide (i.e., focal spot) (Fig. 5(b)), the lens performance significantly increased as it focused the radiation in the x-axis direction. As the lens has such a low permittivity, the phase of the propagating wave does not change much when the wave enters or leaves the lens (Fig. 5(c) and (d)).

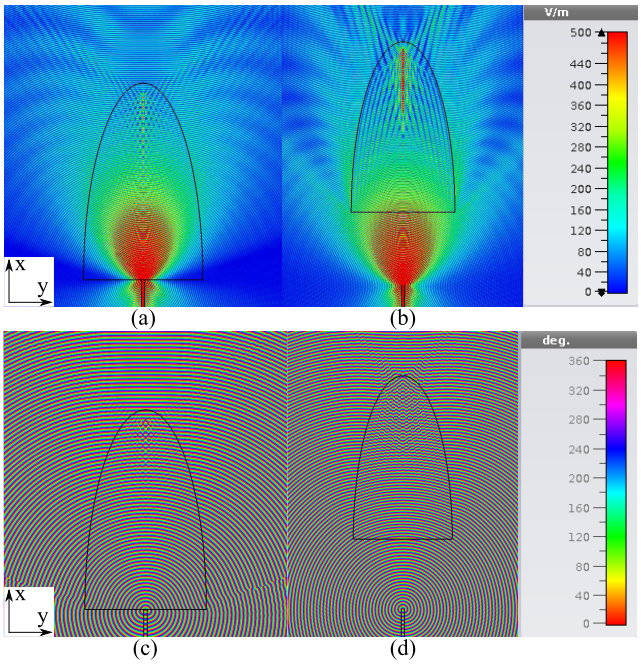


**FIGURE 5.** Simulated near field (E-field) and phase at 300 GHz. (a) When the lens was directly attached to the antenna the lens did not deviate the E-field as much as in (b) when the antenna was at lens focal spot. As the lens has such low permittivity, the phase does not change much at the air-lens interface, (c) and (d).

Simulated broadband 220-330 GHz gain and $S_{11}$ are shown in Fig. 6. There was no need for the matching layer between the feed antenna and the lens because the return loss ($S_{11}$ or reflection coefficient) was better than −10 dB. The bullet lens improved the gain to 25.5-27.5 dBi over the broadband when it was fed at the focal point, compared to the gain values (15.5-17.5 dBi) when it was directly attached to the antenna. Overall, the lens could increase the gain by at least 10 dBi or 20 dBi depending on its distance to the waveguide.

### B. MEASURING THE LENS WITH EXPERIMENTAL SYSTEM

The operation of the lens with the waveguide was studied using an experimental measurement setup. The setup consisted of an N5242B PNA-X (Keysight, USA) connected to frequency extenders operating from 220 GHz to 330 GHz (Virginia diodes, USA). The transmitter (Tx) was connected to an open-ended standard rectangular WR3.4 waveguide and the receiver (Rx) to a standard horn antenna with a gain of 20 dBi shown in Fig. 7.

The Tx and Rx were aligned to face each other at a distance of 520 mm (maximum possible distance between the Tx and Rx) and the lens was positioned between. To move the lens, it was attached to a stepper-motor controlled 3D positioner that could be moved in x-, y- and z-directions between the Tx and Rx.

Two measurements were conducted to analyze the fabricated lens with the proposed measurement system and results are presented for 300 GHz center frequency.

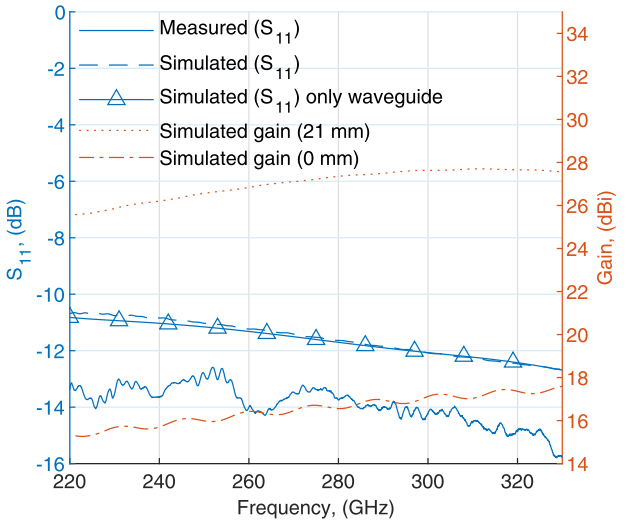


**FIGURE 6.** Broadband characteristics of the bullet shaped lens antenna.

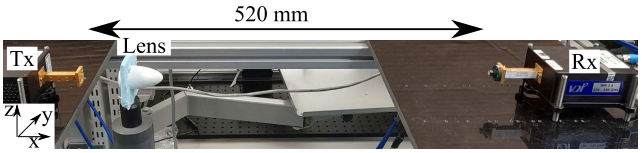


**FIGURE 7.** A photograph of the experimental measurement setup used to characterize the fabricated bullet lens.

The purpose of the first measurement was to determine the position of the lens where the measured $S_{21}$ was at its maximum by moving the lens in the x-direction in 1.5 mm increments and the results are presented in Fig. 8. When the lens was moved away from the Tx, the measured $S_{21}$ increased and reached the highest value around 117 mm distance from the Tx.

The second measurement was conducted to determine the focal spot size in y- and z-dimensions at the highest received signal location which was previously found to be at 117 mm from the Tx. The lens was moved in z- and y-directions by 0.25 mm steps and the measured $S_{21}$ response is shown in the Fig. 9.

The results indicated that the lens had quite a round spot whose width could be estimated to be 1.5 mm (−5 dB). In addition, a second lower intensity "ring" emerged when the lens was moved more than 2 mm from the centerline.

## IV. COMPARISON STUDY

This section presents a comparative study on recently published articles in the field. Several researchers have reported lens antennas for frequencies between 200 GHz and 300 GHz. The most relevant works are collected in Table 1 for comparison at 300 GHz center frequency. This bullet shape lens antenna was able to achieve a very high gain and high bandwidth, and its permittivity was the lowest. In the other words,

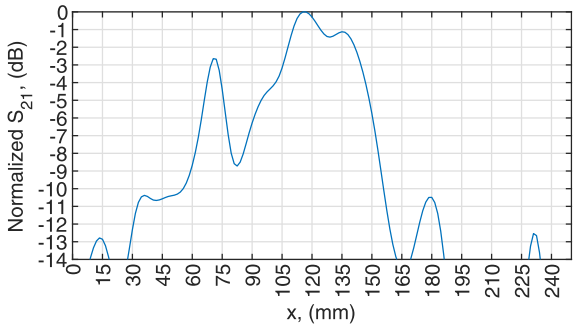


**FIGURE 8.** Measured change in the $S_{21}$ parameter when the lens was moved towards the Rx. Optimal distance was found around 117 mm from the Tx at 300 GHz.

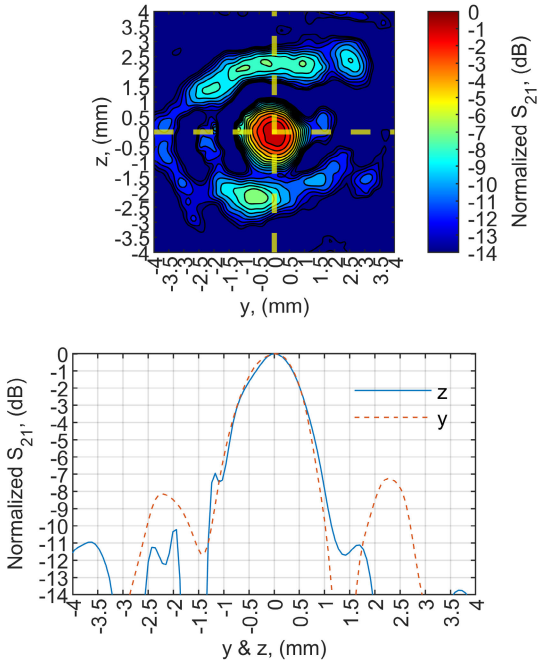


**FIGURE 9.** Measured 2D image when the lens was at optimal distance from the Tx and the focal spot of bullet lens was 1.5 mm (−5 dB) in size at 300 GHz.

Lens antenna made from the LMO-HGMS lens and fed by WR3.4 can perform as equal as those listed in the Table 1.

Additional to the antenna parameters, there is a physical parameter, reflectivity, which tells the perceptual amount of the radiation that is reflected away from the material in the interface of two media; in this case the material-air interface. As the LMO-HGMS composite permittivity is near the permittivity of the air, only 0.2 % of the incident radiation is reflected.

Compared to the other materials it has the lowest reflectivity whereas the most common lens material, silicon, has the highest reflectivity. This issue with high reflectivity with high permittivity materials has been addressed with matching layers which raises the complexity of the lens [34], [35]. With low permittivity materials there is no need to take such a complicated approach in the lens design and fabrication.

**TABLE 1. Comparison study at 300 GHz.**

| Ref | Gain (dBi) | FBW (%) | HPBW (degree) | Material and permittivity ($\varepsilon_r$) | Fabrication method | Lens type | Lens size | Reflectivity (%) | Matching | Lens density (kg/m$^3$) | Lens weigth[1] (g) |
|---|---|---|---|---|---|---|---|---|---|---|---|
| [32] | 21.0 | 12 | - | Silicon 11.9 | Photo-litography | Extended hemipsherical shallow lens | Diameter = 2.5 mm, extension = air gap less than 1 mm | 30 | Iris on aperture layer | 2330 | 16.5 |
| [16] | 30.0 | 37 | 2.5 | Rexolite 3.2 | CNC micro-machining | Extended hemispherical lens with tapered extension | Diameter = 20 mm, extension = 11 mm | 8 | WR 3 | 1050 | 7.4 |
| [17] | 16.0 | 37 | 12 | Monocure 3DR3582C photopolymer 2.8 | 3D printing | Extended hemispherical lens | Diameter = 6 mm, extension = 3 mm | 6 | WR 3 | -[2] | -[2] |
| [33] | 21.2 | 37 | - | Teflon 2.1 | Not given in the paper | Thick lens with both sides curved | Diameter = 10 mm, $r_1$=13.5 mm, $r_2$ =5.5 mm, t=2 mm | 3 | No | 2200 | 15.6 |
| This work | 17.5 or[3] 27.5 | 40 | 2.5 | LMO-HGMS 1.18 | Room Temperature Fabrication of cearmic composites by casting | Bullet shaped lens | Diameter = 30 mm, heigth = 49.5 mm, extension = 0 mm or 21 mm air gap | 0.2 | No | 212.51 | 1.5 |

[1]Calculated for 30 mm half spherical lens for comparison.

[2]Material is UV resin and density and weight of solid object made from such material is unknown to authors at the time of writing this paper.

[3]Depends on the length of the extension, 0 mm or 21 mm.

Also, material density and lens weight are compared. Because the lens may have different optimal shapes for different antennas, a comparison is made for the 30 mm half spherical shape. As previously mentioned, a bullet-shaped lens made from LMO-HGMS weighed only 5 grams, a 30 mm half sphere is much lighter weighing only 1.5 grams and so making objects made from this material ultralight weight compared to other materials listed in Table 1.

## V. CONCLUSION

Lithium molybdenum oxide glass composite was made without high temperature processes, which saves energy and makes manufacturing cheaper and more environmentally friendly.

The composite has a very low permittivity and losses at THz frequency ($\varepsilon_r = 1.18$ and $\tan\delta = 0.003$ at 300 GHz). As the permittivity is such low then the reflectivity from the LMO-HGMS interface is very low (0.2 %), which can be a useful property when the material is used as an RF lens.

Simulated results showed that the proposed waveguide-bullet lens antenna operates at a gain of 27.5 dBi with a narrow beam width of 1-degree, 18 dB SLL and FBW 40% at an operating frequency from 220 GHz to 330 GHz. In addition, it operates with an acceptable reflection coefficient $S_{11}$ below $-13$ dB over the broadband.

The use of LMO-HGMS in various antenna and RF solutions where low permittivity and low losses are useful should be investigated in future.

## REFERENCES

[1] A. Redo-Sanchez, N. Laman, B. Schulkin, and T. Tongue, "Review of terahertz technology readiness assessment and applications," *J. Infr., Millim., THz Waves*, vol. 34, no. 9, pp. 500–518, Sep. 2013.

[2] J. F. O'Hara, S. Ekin, W. Choi, and I. Song, "A perspective on terahertz next-generation wireless communications," *Technologies*, vol. 7, no. 2, p. 43, Jun. 2019.

[3] Z. Chen, X. Ma, B. Zhang, Y. X. Zhang, Z. Niu, N. Kuang, W. Chen, L. Li, and S. Li, "A survey on terahertz communications," *China Commun.*, vol. 16, no. 2, pp. 1–35, Feb. 2019.

[4] T. S. Rappaport, Y. Xing, O. Kanhere, S. Ju, A. Madanayake, S. Mandal, A. Alkhateeb, and G. C. Trichopoulos, "Wireless communications and applications above 100 GHz: Opportunities and challenges for 6G and beyond," *IEEE Access*, vol. 7, pp. 78729–78757, 2019.

[5] M. Matinmikko-Blue, S. Yrjölä, and P. Ahokangas, "Moving from 5G in verticals to sustainable 6G: Business, regulatory and technical research prospects," in *Cognitive Radio-Oriented Wireless Networks* (Lecture Notes of the Institute for Computer Sciences, Social Informatics and Telecommunications Engineering), G. Caso, L. De Nardis, and L. Gavrilovska, Eds. Cham, Switzerland: Springer, 2021, pp. 176–191.

[6] M. Božanić and S. Sinha, "6G networks: Fusion of communications, sensing, imaging, localization and other verticals," in *Mobile Communication Networking: 5G and a Vision 6G* (Lecture Notes in Electrical Engineering), M. Božanić and S. Sinha, Eds. Cham, Switzerland: Springer, 2021, pp. 305–335.

[7] 6G Flagship. *6G Radio THz Sensing Demo*. Accessed: Oct. 9, 2021. [Online]. Available: https://www.youtube.com/watch?v=TL1BcleFORs

[8] M. Kokkonen, H. Juttula, A. Mäkynen, S. Myllymäki, and H. Jantunen, "The effect of drop shape, sensing volume and raindrop size statistics to the scattered field on 300 GHz," *IEEE Access*, vol. 9, pp. 101381–101389, 2021.

[9] M. Caris, S. Stanko, S. Palm, R. Sommer, A. Wahlen, and N. Pohl, "300 GHz radar for high resolution SAR and ISAR applications," in *Proc. 16th Int. Radar Symp. (IRS)*, Dresden, Germany, Jun. 2015, pp. 577–580.

[10] F. Garcia-Rial, D. Montesano, L. Perez-Eijo, M. Arias, B. Gonzalez-Valdes, A. Pino, and J. Grajal, "Evaluation of standoff multistatic 3-D radar imaging at 300 GHz," *IEEE Trans. THz Sci. Technol.*, vol. 10, no. 1, pp. 58–67, Jan. 2020.

[11] S. Chen, Y. Liang, S. Sun, S. Kang, W. Cheng, and M. Peng, "Vision, requirements, and technology trend of 6G: How to tackle the challenges of system coverage, capacity, user data-rate and movement speed," *IEEE Wireless Commun.*, vol. 27, no. 2, pp. 218–228, Apr. 2020.

[12] A. Mourad, R. Yang, P. H. Lehne, and A. de la Oliva, "Towards 6G: Evolution of key performance indicators and technology trends," in *Proc. 2nd 6G Wireless Summit*, Levi, Finland, Mar. 2020, pp. 1–5.

[13] M. Božanić and S. Sinha, "Leap to 6G?" in *Mobile Communication Networks: 5G and a Vision of 6G* (Lecture Notes in Electrical Engineering), M. Božanić and S. Sinha, Eds. Cham, Switzerland: Springer, 2021, pp. 1–29.

[14] R. Piesiewicz, T. Kleine-Ostmann, N. Krumbholz, D. Mittleman, M. Koch, J. Schoebel, and T. Kurner, "Short-range ultra-broadband Terahertz communications: Concepts and perspectives," *IEEE Antennas Propag. Mag.*, vol. 49, no. 6, pp. 24–39, Dec. 2007.

[15] T. Harter, C. Füllner, J. N. Kemal, S. Ummethala, J. L. Steinmann, M. Brosi, J. L. Hesler, E. Brändermann, A.-S. Müller, W. Freude, S. Randel, and C. Koos, "Generalized Kramers–Kronig receiver for coherent terahertz communications," *Nature Photon.*, vol. 14, no. 10, pp. 601–606, Oct. 2020.

[16] K. Konstantinidis, A. P. Feresidis, C. C. Constantinou, E. Hoare, M. Gashinova, M. J. Lancaster, and P. Gardner, "Low-THz dielectric lens antenna with integrated waveguide feed," *IEEE Trans. THz Sci. Technol.*, vol. 7, no. 5, pp. 572–581, Sep. 2017.

[17] N. Chudpooti, N. Duangrit, P. Akkaraekthalin, I. D. Robertson, and N. Somjit, "220-320 GHz hemispherical lens antennas using digital light processed photopolymers," *IEEE Access*, vol. 7, pp. 12283–12290, 2019.

[18] J. Xu, Z. N. Chen, and X. Qing, "270-GHz LTCC-integrated high gain cavity-backed Fresnel zone plate lens antenna," *IEEE Trans. Antennas Propag.*, vol. 61, no. 4, pp. 1679–1687, Apr. 2013.

[19] A. Ghavidel, S. Myllymäki, M. Kokkonen, N. Tervo, M. Nelo, and H. Jantunen, "A sensing demonstration of a sub THz radio link incorporating a lens antenna," *Prog. Electromagn. Res. Lett.*, vol. 99, pp. 119–126, 2021.

[20] M. A. Uusitalo, M. Ericson, B. Richerzhagen, E. U. Soykan, P. Rugeland, G. Fettweis, D. Sabella, G. Wikström, M. Boldi, M.-H. Hamon, H. D. Schotten, V. Ziegler, E. C. Strinati, M. Latva-aho, P. Serrano, Y. Zou, G. Carrozzo, J. Martrat, G. Stea, P. Demestichas, A. Pärssinen, and T. Svensson, "Hexa-X the European 6G flagship project," in *Proc. Joint Eur. Conf. Netw. Commun. 6G Summit*, Porto, Portugal, Jun. 2021, pp. 580–585.

[21] P. Hillger, J. Grzyb, R. Jain, and U. R. Pfeiffer, "Terahertz imaging and sensing applications with silicon-based technologies," *IEEE Trans. THz Sci. Technol.*, vol. 9, no. 1, pp. 1–19, Jan. 2019.

[22] S. D. Liyanaarachchi, C. B. Barneto, T. Riihonen, and M. Valkama, "Experimenting joint vehicular communications and sensing with optimized 5G NR waveform," in *Proc. IEEE 93rd Veh. Technol. Conf.*, Helsinki, Finland, Apr. 2021, pp. 1–5.

[23] R. Sauleau, C. A. Fernandes, and J. R. Costa, "Review of lens antenna design and technologies for mm-wave shaped-beam applications," in *Proc. 11th Int. Symp. Antenna Technol. Appl. Electromagn.*, Saint-Malo, France, Jun. 2005, pp. 1–5.

[24] M. T. Sebastian, R. Ubic, and H. Jantunen, "Low-loss dielectric ceramic materials and their properties," *Int. Mater. Rev.*, vol. 60, no. 7, pp. 392–412, Jul. 2015.

[25] H. Kähäri, M. Teirikangas, J. Juuti, and H. Jantunen, "Dielectric properties of lithium molybdate ceramic fabricated at room temperature," *J. Amer. Ceram. Soc.*, vol. 97, no. 11, pp. 3378–3379, Nov. 2014.

[26] J. Watson and G. Castro, "A review of high-temperature electronics technology and applications," *J. Mater. Sci. Mater. Electron.*, vol. 26, no. 12, pp. 9226–9235, 2015.

[27] H. Kähäri, P. Ramachandran, J. Juuti, and H. Jantunen, "Room-temperature-densified $Li_2MoO_4$ ceramic patch antenna and the effect of humidity," *Int. J. Appl. Ceram. Technol.*, vol. 14, no. 1, pp. 50–55, Jan. 2017.

[28] H. Kähäri, M. Teirikangas, J. Juuti, and H. Jantunen, "Improvements and modifications to room-temperature fabrication method for dielectric $Li_2MoO_4$ ceramics," *J. Amer. Ceram. Soc.*, vol. 98, no. 3, pp. 687–689, 2015.

[29] M. Kokkonen, M. Nelo, J. Chen, S. Myllymäki, and H. Jantunen, "Low permittivity environmentally friendly lenses for Ku band," *Prog. Electromagn. Res. Lett.*, vol. 93, pp. 1–7, 2020.

[30] J.-L. Coutaz, F. Garet, and V. P. Wallace, *Principles of Terahertz Time-Domain Spectroscopy*, 1st ed. Dubai, United Arab Emirates: Jenny Stanford, 2018.

[31] *CST Studio Suite 3D EM Simulation and Analysis Software*. Accessed: Aug. 25, 2021. [Online]. Available: https://www.3ds.com/products-services/simulia/products/cst-studio-suite/

[32] K. Wang and F. Yang, "300 GHz dual-polarized micro-lens antenna for terahertz integrated heterodyne arrays," in *Proc. Int. Workshop Antenna Technol.*, Nanjing, China, Mar. 2018, pp. 1–3.

[33] I. Abdo, T. Fujimura, T. Miura, A. Shirane, and K. Okada, "A 300 GHz dielectric lens antenna," in *Proc. 12th Global Symp. Millim. Waves (GSMM)*, Sendai, Japan, May 2019, pp. 17–19.

[34] C. Apriono, A. P. Aji, T. Wahyudi, F. Zulkifli, and E. T. Rahardjo, "High-performance radiation design of a planar bow-tie antenna combined with a dielectric lens and cascaded matching layers at terahertz frequency," *Int. J. Technol.*, vol. 9, no. 3, p. 589, Apr. 2018.

[35] P. Van Hung, N. Q. Dinh, H. D. Thuyen, N. T. Hung, L. M. Thuy, L. T. Trung, and Y. Yamada, "Estimations of matching layers effects on lens antenna characteristics," in *Industrial Networks and Intelligent Systems* (Lecture Notes of the Institute for Computer Sciences, Social Informatics and Telecommunications Engineering), vol. 334, N.-S. Vo and V.-P. Hoang, Eds. Cham, Switzerland: Springer, 2020, pp. 85–94.

**MIKKO KOKKONEN** received the bachelor's and master's degrees in physics from the University of Oulu, Oulu, Finland, where he is currently pursuing the Ph.D. degree with the Microelectronics Research Unit, Faculty of Information Technology and Electrical Engineering. His current research interest includes the use of new materials as an RF lens. He is also interested in solar panels and green energy.

**ALI GHAVIDEL** received the Ph.D. degree from the Polytechnic University of Catalonia (UPC), Barcelona, Spain. Since 2015, he has been working on circuit device developing for millimeter and terahertz technology. He is currently working as a Researcher with the Microelectronic Research Unit, University of Oulu, Finland.

**NUUTTI TERVO** (Member, IEEE) received the B.Sc. (Tech.) and M.Sc. (Tech.) degrees in electrical engineering from the University of Oulu, Oulu, Finland, in 2014, where he is currently pursuing the Ph.D. degree with the Centre for Wireless Communications (CWC). His Ph.D. dissertation research focuses on nonlinearity and linearization of millimeter-wave beamforming transceivers. He has a strong background in different fields of wireless communications, including radio frequency (RF), radio channel modeling, signal processing, and system-level analysis. Around those topics, he has already authored or coauthored more than 45 international journal articles and conference papers and holds patents. In 2019, he was a recipient of the Young Scientist Award of the URSI XXXV Finnish Convention on Radio Science, Tampere.

**MIKKO NELO** received the M.Sc. degree in organic chemistry and the D.Sc. degree in electrical engineering from University of Oulu, in 2005 and 2015, respectively. He has 29 peer-reviewed publications and ten patents or pending patents. His current research interests include ceramic composite materials, ultra-low permittivity materials, and formulation of printed electronics inks.

**SAMI MYLLYMÄKI** received the M.Sc. and D.Sc. degrees from the University of Oulu, Oulu, Finland. He is currently a Research Group Leader and an Adjunct Professor with the Microelectronics Research Unit, Faculty of Information Technology and Electrical Engineering, University of Oulu. His research interests include microwave measurements, components, and materials, and teaching includes electronics packaging technology.

**HELI JANTUNEN** has been the Group Leader of the Electronics Materials, Packaging and Reliability Techniques Research Group, Infotech Oulu, Finland, since 2004. She is currently a Professor and the Head of the Microelectronics Research Unit, Faculty of Information Technology and Electrical Engineering, University of Oulu, Oulu, Finland. Her current research interests include the design, development, synthesis, and implementation of electronics materials and their components for RF and microwave applications, as well as multifunctional micromodules.